Petroleum Science 20 (2023) 3337–3347

Contents lists available at ScienceDirect

Petroleum Science

journal homepage: www.keaipublishing.com/en/journals/petroleum-science

Original Paper

Mechanism of ultrasonic strengthening fluidity of low mature shale oil: A case study of the first member of Lucaogou Formation, western Jimusaer Sag, Northwest China

Bo-Yang Wang [a], Bo Liu [a, *], Yun-Fei Cui [a], Zi-Long Wang [b]

[a] Key Laboratory of Continental Shale Hydrocarbon Accumulation and Efficient Development, Ministry of Education, Northeast Petroleum University, Daqing, 163318, Heilongjiang, China
[b] No.203 Exploration Team, Jilin Bureau of Coalfield Geology, Siping, 136000, Jilin, China

ARTICLE INFO

Article history:
Received 8 October 2022
Received in revised form
22 December 2022
Accepted 20 August 2023
Available online 21 August 2023

Edited by Jie Hao and Teng Zhu

Keywords:
Ultrasonic
Shale oil
Reservoir properties
Mobility
Recovery

ABSTRACT

The low mature shale oil resources of Lucaogou Formation in Jimusar Sag have a great potential, but the heavy oil quality limits large-scale economic development significantly. Ultrasonic is a typical representative of heavy oil viscosity reduction and anhydrous fracturing technology, and how to understand the action characteristics and mechanism of ultrasonic effect on reservoir is a critical issue to enhance shale oil production in the industrialized application of power ultrasonic. Therefore, the comparative experiments with different time of power ultrasonic loading were conducted to analyze the response mechanism of reservoir characteristics and the change of fluid mobility. The results indicate that the ultrasonic treatment is ameliorative to the pore-fracture structure, and the improvement degree is controlled by the mechanical vibration and cavitation of ultrasound. Generally, the location with weak cementation strength or relatively developed microcrack is preferred to pore expansion. After the ultrasonic treatment, the shale oil quality becomes lighter, and the transformation of shale oil from adsorbed to free, is accelerated due to enhanced fluidity. Pore-expanding effect and fluid mobility enhancement are essential aspects of the power ultrasonic loading to improve the recovery of low mature shale oil. The results of this study support the feasibility analysis of ultrasonic enhanced shale oil exploitation theoretically.

1. Introduction

Lucaogou Formation in Jimusar Sag is one of the most successful unconventional reservoirs in exploration and development of China. Almost 1.2 billion tons of shale oil resources have been found, which has the typical characteristics of source-reservoir integration, complex lithology, large-area frequent interbedding etc. At present, 30 horizontal wells and 40 vertical wells have been drilled in this region with a daily oil production of 388.4 t/d and a cumulative oil production of 2.292×10^5 t, showing great exploration and development potential (Peng et al., 2021a,b). However, the current production capacity is mainly contributed by the flowable medium hydrocarbons in the pore throats above 300 nm. The heavy oil in the pore throats of 50–300 nm is difficult to use, which greatly limits its large-scale economic development (Wang et al., 2021a). Previous studies have shown that the source rocks of Lucaogou Formation are in a generally salty reduction environment, and aquatic organisms, such as algae, are developed (Liu et al., 2018). A large number of hydrocarbons are generated in the low maturity stage, with high content of colloid and asphaltene. Due to short-range migration, the above components are not adsorbed by the rock and remain in the crude oil. Therefore, the oil saturation in that spot is relatively high, but the overall heavy oil quality and poor fluidity are still bottlenecks restricting oil recovery (Wang et al., 2021b).

At present, the most effective and direct way to increase productivity is hydraulic fracturing, which, however, brings along the accompanying environmental problems. Compared with traditional hydraulic fracturing, ultrasonic technology not only has the characteristics of strong applicability, simple operation and low

* Corresponding author.
E-mail address: liubo@nepu.edu.cn (B. Liu).

https://doi.org/10.1016/j.petsci.2023.08.022

cost, but also has the advantages of long effective period stimulation and reducing reservoir damage caused by water rock reaction (Mullakaev et al., 2015; Wang and Xu, 2015; Wang et al., 2020). Understanding the action and mechanism of ultrasonic oil recovery on the reservoir is the key to improve the geological applicability and effectiveness of ultrasonic technology, and it is also the critical problem that needs to be solved in the industrialized application of ultrasonic enhanced shale oil exploitation technology.

The essence of ultrasonic oil recovery is to generate a large energy wave to change some states of crude oil and even reservoir itself to enhance oil recovery. When the ultrasonic wave is transmitted through the medium, it will produce a train of secondary effects, including mechanical effect, thermal effect, cavitation effect and so on, which will alter the crude oil properties and bring down its viscosity (Wang and Xu, 2015; Razavifar and Qajar, 2020). The permeability of the core polluted by drilling fluid has been significantly improved by using ultrasonic with different frequencies (Wang et al., 2020). Zhang and Li (2017) showed that the ultrasonic cavitation effect significantly increased the number of reservoir fractures, and then increased the permeability by 30%–60%. Shi et al. (2017) showed that the stress concentration of ultrasonic waves on the crack tip generated periodic tensile and compressive stresses to promote crack propagation, and the cracks growth path treatment of ultrasonic was studied on combination of physical experiments and numerical simulation (Wang et al., 2022a,b,c). The results showed that the fracture could be split into crack growth zone and instant rift zone. According to the analysis of fracture characteristics, the crack growth mechanism under ultrasonic waves contained fatigue break, surface shear and friction, and heating effect. Peng et al. (2021a,b) proposed that the falling off of mineral particles and the rupture of mineral crystal together promoted rock breakdown under the action of ultrasonic. A large amount of micro-cracks and pores were formed on the eroded rocks surface, which were more conducive to fluid flow. In addition, ultrasonic waves have a significant effect on removing asphaltene deposition around the wellbore and reducing water sensitive damage (Wang and Huang, 2018; Otumudia et al., 2022).

Previous scholars have carried out a lot of research on the propagation characteristics of ultrasonic waves in unconventional reservoirs, such as improving the properties of crude oil, reservoir permeability enhancement, fracture mechanism and so on (Tang et al., 2016; Shi et al., 2019; Chen et al., 2021; Dehshibi et al., 2019). At the same time, the following problems still need to be further addressed: 1) Ultrasonic technology is very mature in the field of viscous oil reduction, and the viscosity of thickened oil will be greatly reduced after ultrasonic treatment(Gopinath et al., 2006; Pawar et al., 2014). However, the original formation conditions are not considered, that is, how the fluid properties change before and after the ultrasonic effect under reservoir constraints is unknown. 2) A large number of experiments have proved that ultrasonic waves are useful for ameliorating the reservoir physical properties. The vibration process makes the reservoir compress and expand, and the internal friction coefficient and bonding force between particles are reduced, which plays a role in expanding pores and increasing permeability (Karr et al., 2017; Shi et al., 2017; Zhang and Li, 2017). However, most of the current researches only focus on coal reservoirs. The macro fracture propagation law and micro pore response law of shale oil reservoir under the effect of ultrasonic machinery are not clear. 3) It is not clear how the change of reservoir surface properties and the variation of fluid properties under ultrasonic effect affect shale oil recovery and its mechanism.

On account of the above issues, the oil-saturated samples were taken from the lower sweet spot of the first member of the Lucaogou Formation ($P_2l_1^2$) in western Jimusaer sag of Junggar Basin. The shale oil in this area is relatively heavy, and the lower sweet spot ($P_2l_1^2$) shale oil is heavier and thicker than the upper sweet spot ($P_2l_2^2$) shale oil. The average density of shale oil in $P_2l_2^2$ is 0.8836 g/cm^3, and the average viscosity is 41.7 mPa·s at 50 °C. The average density of shale oil in $P_2l_1^2$ is 0.9062 g/cm^3, and the average viscosity is 154.6 mPa·s at 50 °C (Li et al., 2020a,b). Therefore, it is critical for shale oil development in this district to find the way to increase the mobility of crude oil of $P_2l_1^2$. In order to analyze the response mechanism of physical and chemical properties of shale oil reservoir under the power of ultrasonic waves, a physical simulation experiment of pore-fracture characteristics, crude oil quality characteristics, spontaneous imbibition law and its impact on displacement efficiency were carried out. Finally, the mechanism of ultrasonic strengthening the fluidity of low mature shale oil was revealed.

2. Geological setting

Jimusar sag is situated in the eastern margin of Junggar basin. It is a dustpan shaped sag with faults in the west and superimposition in the east developed on the middle Carboniferous fold basement (Fig. 1a-c). Lucaogou Formation of Permian is an important oil-bearing series in the sag, which is divided by P_2l_1 and P_2l_2 from bottom to top. It is consisted of mixed fine-grained sediments of fine-grained silty sandstone, carbonate and mudstone with the synactic action of mechanical deposition, biological deposition and chemical deposition in the saline lake environment. The main lithology includes siltstone, mudstone, dolomite and dolomitic siltstone (Xiao et al., 2021). Lucaogou Formation develops upper and lower sweet spots which are respectively located in the upper part of P_2l_1 and P_2l_2. The dominant reservoir lithology of upper sweet spot is mainly siltstone, argillaceous siltstone and sand debris, and the dominant reservoir lithology of lower sweet spot is siltstone (Fig. 1d).

3. Samples and methods

3.1. Samples

In this study, oil saturated samples from $P_2l_2^2$ with a buried depth of 4623.6 m in well J-X were collected by closed coring (Fig. 1). The test can be segmented into two portions: one is the sample basic test, and the other is the series test under the ultrasonic effect, mainly including pore-fracture evolution test, shale oil occurrence state transition test, fluid-solid interface properties change test and imbibition displacement test. The samples used follow the principle of parallel sample preparation.

3.2. Methods

3.2.1. Basic characteristic test

Mineral compositions were tested through X' Pert-MPD diffraction instrument. Samples were pulverized to 200 mesh (Li et al., 2020a,b). The relative mineral percentages were calculated in terms of the reference intensity ratio method. The total organic carbon (TOC) content was carried out by LECO CS230HC analyzer. The inorganic carbon was removed by dilute hydrochloric acid, and the rest is organic carbon (Li et al., 2016). The pyrolysis test was carried out by Rock Eval VI instrument to obtain S_1, S_2, S_3, T_{max}) (Li et al., 2020a,b; Bai et al., 2022). OSI (oil saturation index) was the ratio of ($S_1 \times 100$) to TOC.

3.2.2. Experiments under the ultrasonic effect

The ultrasonic experimental device is shown in Fig. 2, which is mainly composed of an ultrasonic generator and an ultrasonic transducer. The maximum power of the ultrasonic generator is

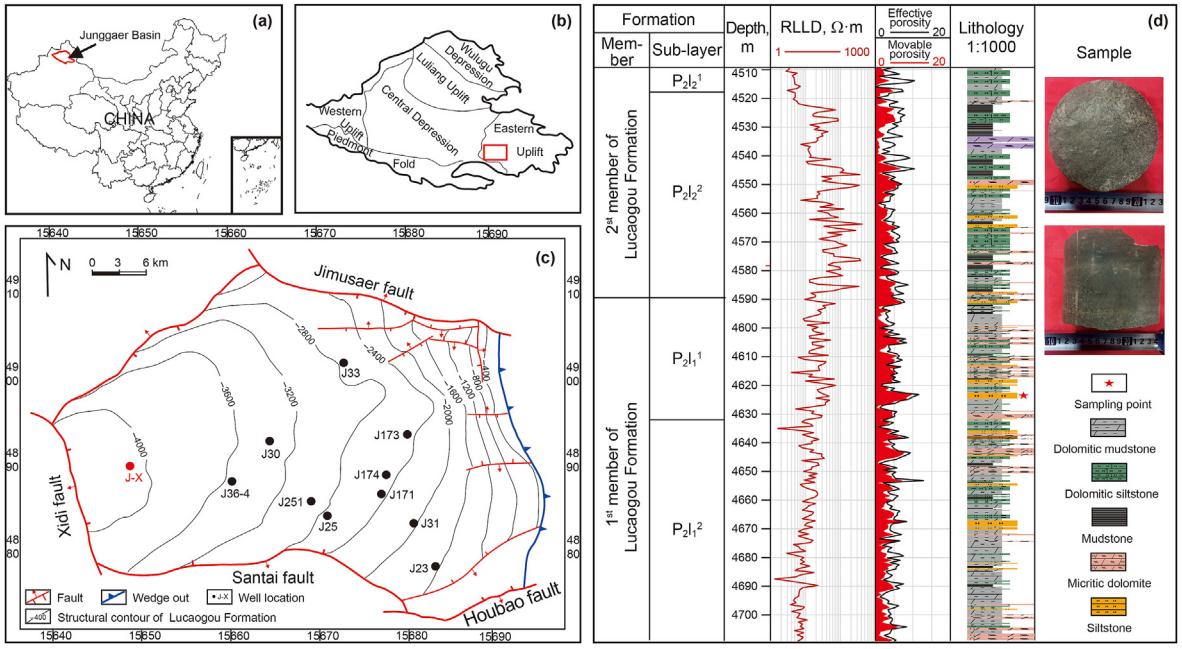

Fig. 1. Geological overview of study area and sampling point information.

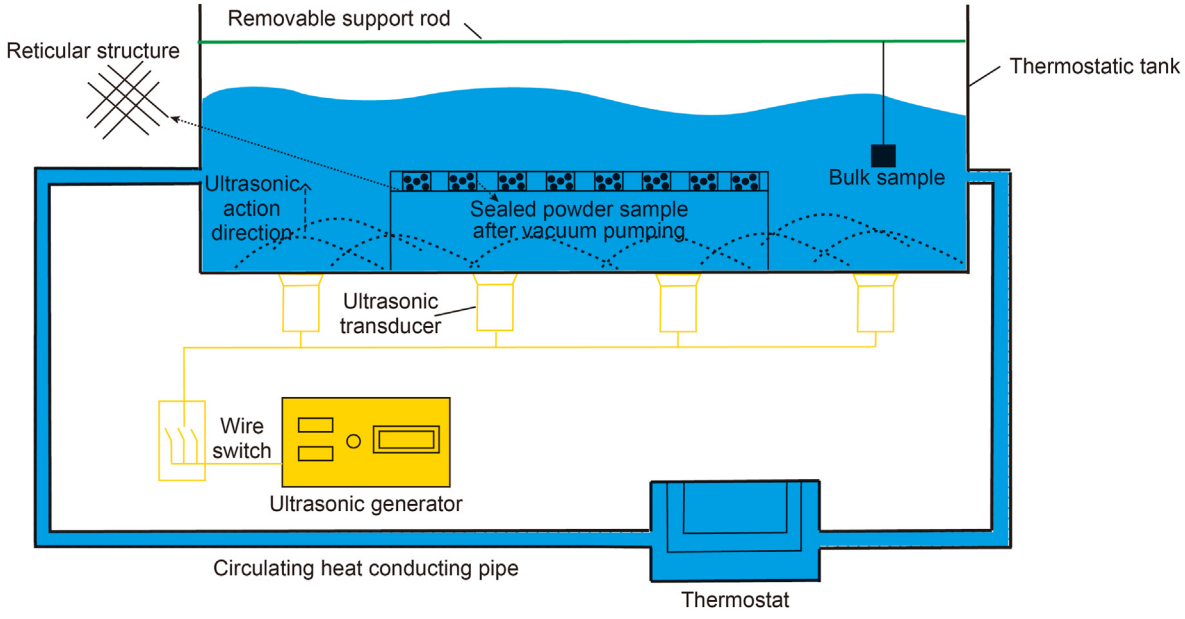

Fig. 2. Ultrasonic experimental device (modified from Shi et al., 2019).

5 kW, and the frequency range of the ultrasonic transducer is 20–50 kHz. The ultrasonic generator is connected with the ultrasonic transducer through circuit. The ultrasonic transducer can convert the input electric power into mechanical power and then transmit it. The transducer is located at the bottom of the machine and the ultrasonic waves propagate from the bottom to the top. Due to the thermal effect and mechanical vibration effect caused by the ultrasonic effect, the refrigeration thermostat is connected externally to ensure that the water temperature in the thermostatic tank is kept at a constant temperature (Shi et al., 2019). Considering the actual formation conditions, the temperature is constant at 60 °C. The ultrasonic parameters are frequency (50 kHz) and sound intensity (10 kW/m^2).

3.2.2.1. Pore-fracture test. In order to analyze the change of macro pore-fracture of shale oil reservoir under ultrasonic treatment, small pieces of 2 cm (length) × 2 cm (height) × 1 cm (width) were obtained along the bedding direction adopting the wire cutting method. Select the direction along the bedding plane as the direction of ultrasonic, put it into the ultrasonic experimental device, and conduct in-situ SEM observation after acting for 0 h, 100 h and 200 h respectively. The instrument used is TESCAN VEGA S5000 tungsten filament scanning electron microscope, and EDAX AMETEK energy spectrometer is used for energy spectrum surface scanning (Cao et al., 2019).

For the purpose of analyzing the changes of nano-scale pores under ultrasonic treatment, the samples were prepared into

Table 1
Basic information of the selected sample.

Selected sample	Mineral composition, %								
	Quartz, %	Plagioclase, %	Calcite, %	Potash feldspar, %	Pyrite, %	Clay minerals	Clay minerals		
							Chlorite	C/S	I/S
	13.5	57.9	17	4.7	1.9	5	19	77	4
	Geochemical parameters								
	TOC, %	T_{max}, °C	S_1, mg/g	S_2, mg/g	S_3, mg/g	OSI, mg/g·TOC			
	0.92	424	1.79	3.70	0.46	194.57			

Note: C/S - chlorite/smectite mixed layer mineral, I/S - illite/smectite mixed layer mineral.

powder with particle size between 0.18 and 0.25 mm, which was divided into 5 parts. Then put it into a sealed bag and vacuum it. Using the Autosorb iQ2 automatic gas adsorption analyzer, nitrogen adsorption experiments were carried out after ultrasonic treatment for 0, 50, 100, 150, 200 h (Wang et al., 2022a,b,c).

3.2.2.2. 2D NMR experiment. A cylindrical sample (2.5 cm in diameter × 5 cm in length) was obtained along the bedding direction. After ultrasonic treatment for 0, 50, 100, 150 and 200 h, the NMR instrument with the experimental frequency of 23 MHz was applied to characterize hydrocarbon fluid and organic matter in samples. The advantage of 2D NMR is able to delimit T_1-T_2 map into four portions, which are crude oil ($T_2 > 0.2$ ms and $T_1 > 10$ ms), solid organic matter ($T_1 > 10$ ms and $T_2 < 0.2$ ms), hydroxyl-rich compound ($T_2 < 0.2$ ms and $T_1 < 10$ ms) and water ($T_1 < 10$ ms and 1 ms $> T_2 > 0.2$ ms) (Wang et al., 2021b).

3.2.2.3. Spontaneous imbibition experiment. Five small pieces with 2 cm (height) × 1 cm (length) × 1 cm (width) were obtained along the bedding direction. The samples were sealed with epoxy resin, and the suction surfaces were polished with different mesh sandpapers. After acting in the ultrasonic experimental device for 0 h, 50 h, 100 h, 150 h and 200 h, it was put into the imbibition device for one-dimensional spontaneous imbibition experiment. By

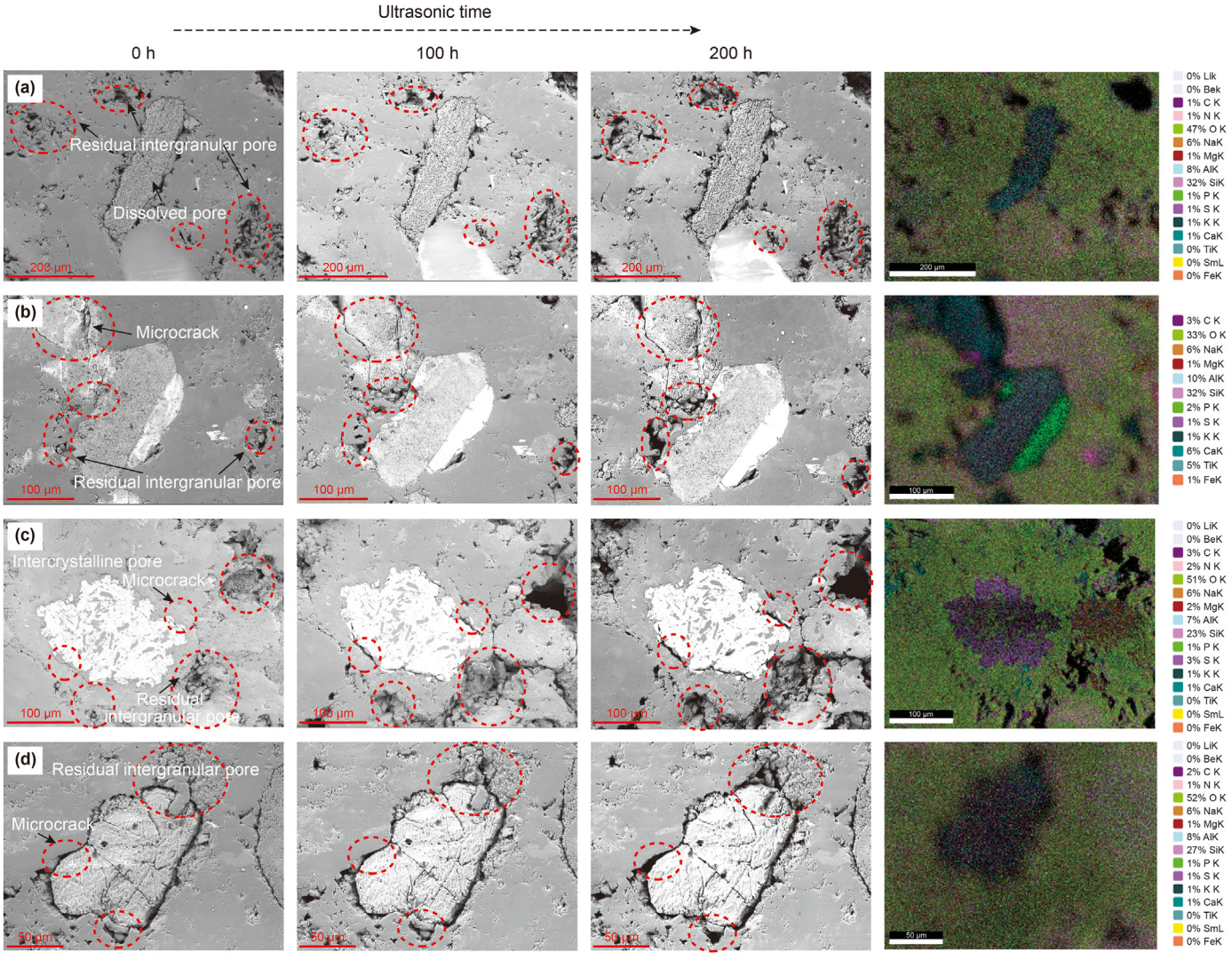

Fig. 3. SEM images of samples under ultrasonic effect.

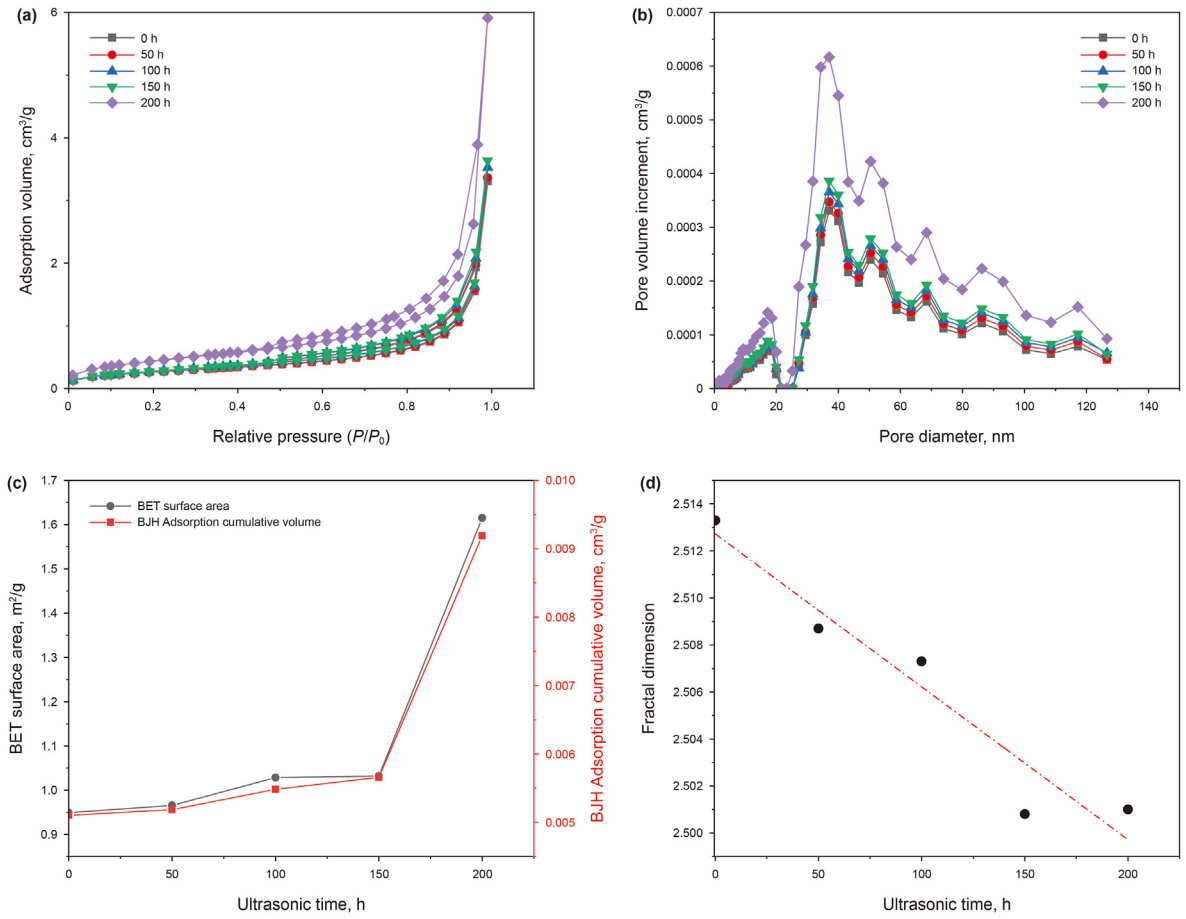

Fig. 4. Changes in pore characteristics under the ultrasonic effect for different time. (a) Relationship between adsorption volume and relative pressure (b) Pore size distribution (c) BJH adsorption volume and BET specific surface area change with ultrasonic time (d) Fracal dimension change with ultrasonic time.

recording the change of sample weight over different time periods, the spontaneous imbibition rate was calculated, and then the changes of liquid-solid interface properties after different time of ultrasonic effect were compared.

3.2.2.4. Oil displacement experiment. Three cylindrical samples (2.5 cm in diameter × 5 cm in length) were obtained along the bedding direction. After acting in the ultrasonic experimental device for 0 h, 100 h and 200 h, the imbibition oil displacement experiments were carried out. First, the samples were vacuum and saturated with *n*-decane, and then deuterium oxide was used for imbibition displacement. After the displacement time was 0 h, 3 h, 6 h, 9 h, 12 h, 24 h and 48 h, the nuclear magnetic T_2 spectrum of the target core were detected, and then the oil displacement efficiency was calculated.

4. Results

4.1. Sample basic information

The selected siltstone sample is mostly made up of plagioclase, contains a certain amount of calcite and quartz, and, to a lesser extent, clay mineral content. The TOC content is low (Table 1). The OSI index is 194.57 mg/g·TOC, suggesting that the crude oil has certain mobility.

4.2. Physical properties of shale oil reservoir under the ultrasonic effect

4.2.1. Macro pores and microcracks

The reservoir structures of this sample are mainly residual intergranular pores, intercrystalline pores, dissolved pores and microcracks (Fig. 3). The residual intergranular pores and microcracks have an increasing trend under the ultrasonic effect. This kind of pore-expanding effect has certain inheritance, which is mainly reflected the fact that the more developed the original pores and microcracks or different mineral cementation are, the easier to form larger pores or fractures under the ultrasonic treatment. This kind of pore-expanding effect is mainly due to the shedding of siliceous minerals, and has obvious time effect. The longer the ultrasonic action time is, the more significant the pore-expanding effect is. However, for complete and hard single minerals (such as dissolved pores in calcite or intercrystalline pores in pyrite), the improvement effect of pore-expanding under the ultrasonic waves is not significant (Fig. 3) (Sahinoglu and Uslu, 2015).

4.2.2. Nano-scale pores

Nitrogen adsorption experiments were used to explore the nano-pore change characteristics of shale oil reservoir under the ultrasonic effect for different time. The results showed that under the action of the ultrasonic mechanical vibration, the pore morphology did not change significantly with the increase of ultrasonic time. The overall pore morphology was still dominated by open pores, which could form adsorption loops, covering

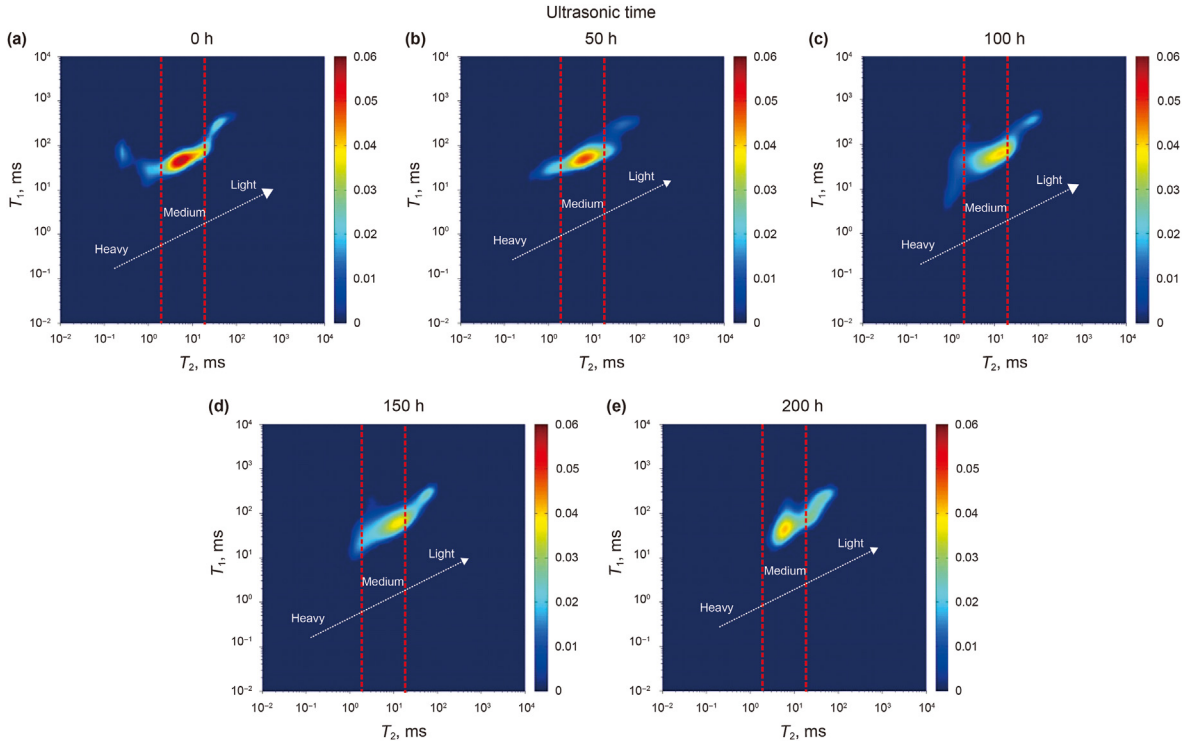

Fig. 5. T_1-T_2 NMR map under different ultrasonic time. (a) 0 h (b) 50 h (c) 100 h (d) 150 h (e) 200 h.

cylindrical pores with two ends open and parallel plate pores with four open (Fig. 4a). Previous studies showed that compared with other pore morphology, the cylindrical pore was more effective under the ultrasonic effect (Otumudia et al., 2022).

When the ultrasonic time was less than 150 h, the pore diameter, BET specific surface area, total pore volume of BJH increased slightly with the increase of ultrasonic time. When the ultrasonic time was 200 h, there was a significant increasing trend (Fig. 4b-c). For the pore size, when the ultrasonic time was less than 150 h, the main increased pore size was concentrated between 40 and 130 nm. When the ultrasonic action time was 200 h, the pore volume at all pore size ranges (0–130 nm) increased. In order to explore the changes of the complexity and roughness for the pore surface of the sample after the ultrasonic effect, the FHH model was used to calculate the fractal dimension (Wang et al., 2022a,b,c). The results showed that the ultrasonic time was negatively correlated with the fractal dimension of the pore, indicating that the pore connectivity of reservoir was gradually improved after ultrasonic mechanical vibration (Fig. 4d).

4.3. Fluidity characteristics of shale oil under ultrasonic effect

Previous studies showed that 2D NMR experiment could effectively divide T_1-T_2 diagram into four parts, which were solid organic matter ($T_1 > 10$ ms and $T_2 < 0.2$ ms), crude oil ($T_2 > 0.2$ ms and $T_1 > 10$ ms), hydroxyl-rich compound ($T_2 < 0.2$ ms and $T_1 < 10$ ms) and water ($T_1 < 10$ ms and 1 ms $> T_2 > 0.2$ ms) (Wang et al., 2021b). The selected sample was oil-rich siltstone, and the fluid signal was mainly distributed in the crude oil (Fig. 5). The larger the values of T_1 and T_2 were, the lighter the oil quality, and the stronger the fluid mobility were. In order to distinguish the relative weight of crude oils more carefully, the quality of crude oil was divided into three parts: heavy (0.2 ms $< T_2 <$ 2 ms), medium (2 ms $\leq T_2 <$ 20 ms) and light ($T_2 \geq$ 20 ms) (Liu et al., 2019). With the increase of ultrasonic vibration time, the fluid signal shifts to the upper right side, indicating that the crude oil quality changes from medium-heavy to light. The overall fluidity was enhanced i.e., the adsorbed crude oil changed to the free crude oil. The mechanism was explained in Section 5.2.

4.4. Fluid-solid interface properties of shale oil reservoir under ultrasonic effect

The essence of spontaneous imbibition was the process of replacing the nonwetting phase with the wetting phase in porous media. There were many factors affecting spontaneous imbibition, such as reservoir physical properties, clay mineral content, fluid properties, etc. Spontaneous imbibition experiment is the main method to study the imbibition of porous media. Spontaneous imbibition experiments were carried out on the samples after ultrasonic treatment over different time periods. The results showed that the law of imbibition curves of different samples was generally the same, which can be divided into three stages: initial imbibition stage, transition imbibition stage and approximate stable stage. In the initial imbibition stage, the infiltration rate was high, and the infiltration volume increased rapidly with the infiltration time. At this time, the infiltration fluid in the capillary was less, and the gravity and viscous force could be ignored. The capillary force and inertial force played the main role. In the transition imbibition stage, the imbibition rate began to decrease significantly, mainly because of the increase of core imbibition volume and the increase of gravity and viscous force of fluid, which slowed down the increase of imbibition. In the approximate stable stage, the imbibition amount tended to be stable with the decrease of fluid imbibition speed. The resultant force of fluid tended to zero, the inertial force weakened, and the infiltration was mainly affected by capillary force and viscous force. The spontaneous imbibition sloped at different stages were positively correlated with the ultrasonic time (Fig. 6b-d). It indicates that the pore connectivity of the reservoir was enhanced under the ultrasonic effect, which increases the

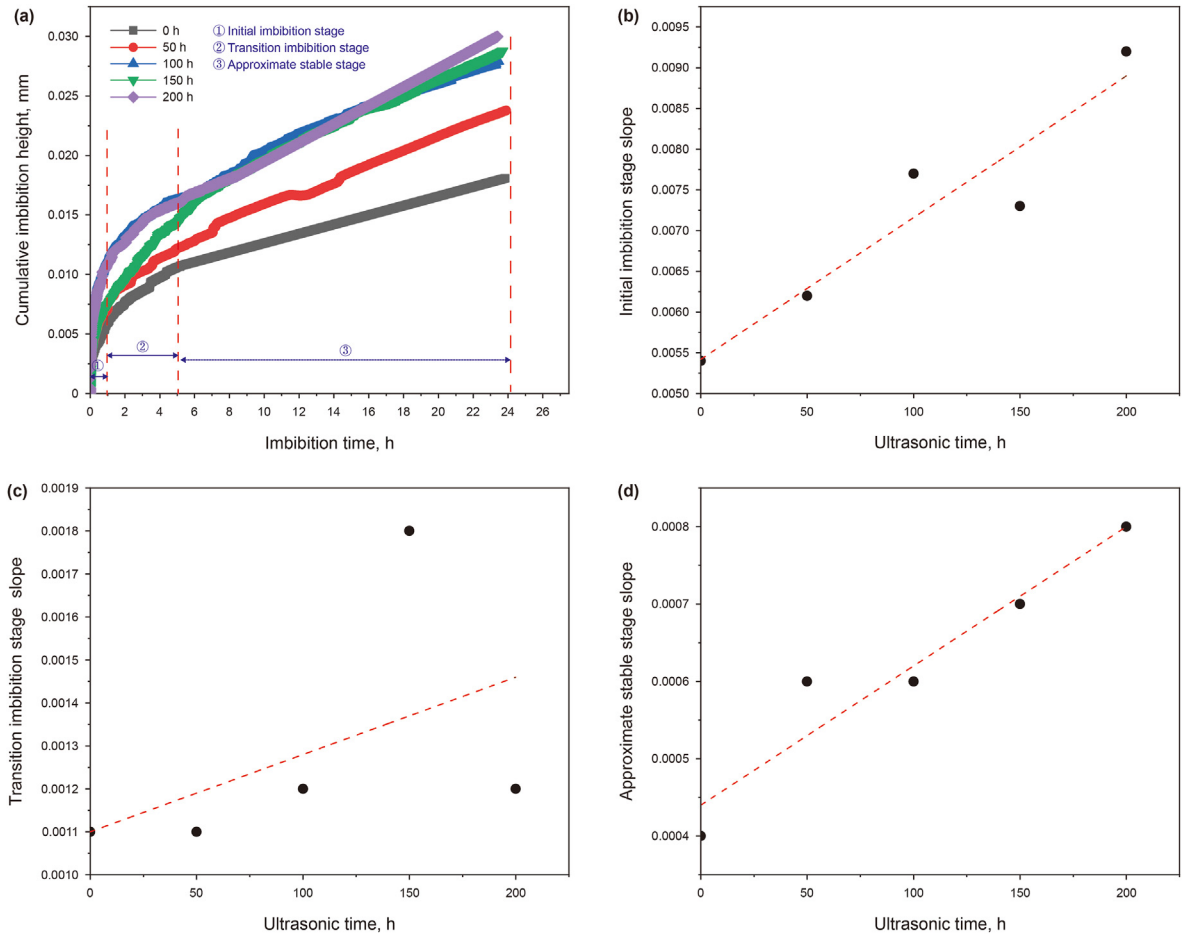

Fig. 6. Spontaneous imbibition characteristics under the ultrasonic effect for different time. (a) Relationship between cumulative imbibition height and imbibition time, (b)-(d) Relationship between slope of different stages and ultrasonic time.

permeability and water wettability of the reservoir.

4.5. Imbibition displacement efficiency of shale oil reservoir under ultrasonic effect

Because shale oil reservoir generally has the characteristics of low porosity, low permeability and mainly water wettability, imbibition displacement is one of the important means for the development of such reservoirs. The imbibition displacement experiments of samples after the ultrasonic were carried out to explore the impact of the ultrasonic effect on shale oil reservoir imbibition displacement efficiency. The results showed that the recovery rate of samples by imbibition was significantly increased after ultrasonic treatment. The relatively large pore range (corresponding to T_2 between 20 ms and 100 ms) had rapid signal attenuation, indicating that the oil droplets in the large pores were discharged preferentially, and the oil displacement rate in small pores were relatively low (Fig. 7). The mechanism was explained in Section 5.2.

5. Discussion

5.1. Improvement mechanism of shale oil reservoir physical properties under ultrasonic

According to the results in sections 4.2 and 4.4, it is observed that the pore and fracture of shale oil reservoir will increase (Liu et al., 2020), and the pore connectivity will be enhanced after the ultrasonic treatment. It is mainly reflected in the positive correlation between the ultrasonic action time and the pore size, BJH pore volume and BET specific surface area, negative correlation with pore fractal dimension (Figs. 3 and 4) and positive correlation with spontaneous infiltration slope (Fig. 6), indicating that the reservoir physical properties have been significantly improved after ultrasonic action.

The main functions of the ultrasonic treatment include mechanical vibration, cavitation effect and thermal effect, of which the first two are the main controlling factors to improve reservoir physical properties (Pu et al., 2011). The physical property improvement mechanism of shale oil reservoir under the ultrasonic waves mainly includes: 1) Mechanical vibration effect: the mechanical vibration of the ultrasonic waves will cause alternating vibration of rock particles. The rock particles at the interface are easy to loosen due to uneven stress, especially, some particles with weak cementation. It can be clearly seen by SEM that the pore-expanding effect is mainly due to the shedding of siliceous mineral particles (Fig. 3). For sedimentary rock, the strength of cementation between mineral particles is significantly lower than that of mineral particles. Under the action of mechanical vibration, the rock cementation structure is destroyed, the mineral particles will peel off from the rock mass, and the peeled particles will form erosion pits. With the increase of the ultrasonic treatment time, the adjacent pits merge and form larger macroscopic erosion pits. This explains why the pore-expanding effect in a single particle is

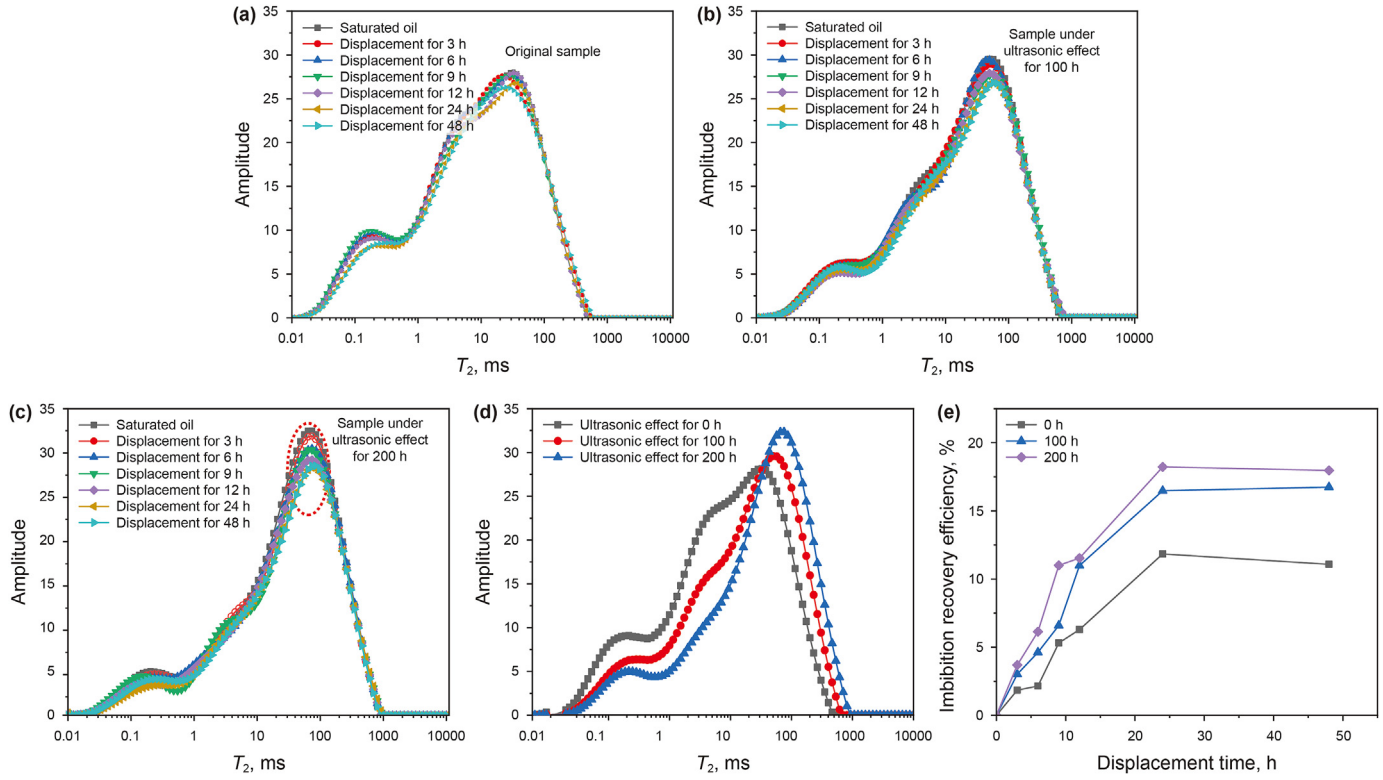

Fig. 7. Imbibition displacement characteristics under the ultrasonic effect for different time. (a)-(c) NMR T_2 spectra of different displacement time for samples under different ultrasonic effect time (d) Saturated oil NMR T_2 spectra of samples under different ultrasonic time (e) Relationship between imbibition recovery efficiency and displacement time.

significantly lower than that at the cementation between particles (Peng et al., 2021a,b). In addition, the particle motion caused by high-frequency vibration has a large acceleration and a great kinetic energy, thus impacting and damaging the microstructure of rock. If the energy is large enough, a series of microcracks will be formed near the mechanical weak surface. 2) Cavitation effect: The energy of the cavitation bubble collapse can produce pores and fractures, and this cavitation erosion has a more significant effect on the damaged surface. This also explains why the more developed the fracture position of the original sample is, the easier it is to form larger pores or fractures under the action of the ultrasonic waves (Dular and Osterman, 2008). The main reason is that the developed microcracks and pores are the preferred mechanical weak surfaces of cavitation erosion. With the increase of the ultrasonic cavitation erosion time, a large number of microcracks and pores are connected to form a connected three-dimensional pore-fracture network, which improves the pore connectivity of the reservoir. 3) Fatigue damage effect: The ultrasonic waves act on the sample in the form of high frequency and high cycle fatigue loading (Liu and Dai, 2021). This elastic wave can be distinguished into a transverse wave parallel to the internal crack surface and a longitudinal wave perpendicular to the internal crack surface, which is usually transmitted in the form of a longitudinal wave. The longitudinal wave repeatedly opened and closed pores and fractures in a period, resulting in fracture propagation in plane. The longer the ultrasonic treatment time is, the more significant the fatigue damage effect is. 4) Frictional failure effect: Under the ultrasonic high-frequency alternating load, the crack tip expands, and the crack contact surface suffers severe friction. Rock particles are easy to loosen and fall off, resulting in the increase of pores and cracks. In addition, friction heating has also been proved to be easier to induce rock damage (Wang et al., 2022a,b,c) (Fig. 8).

5.2. Mechanism of improving shale oil recovery under the ultrasonic treatment

The improvement of shale oil recovery by power ultrasound is mainly reflected in the following two aspects.

5.2.1. Reduce viscosity and promote flow

Shale oil is mainly in free and adsorbed state in the reservoir. The former has strong fluidity and mainly exists in macropores and microcracks. The latter has poor fluidity and is composed of medium-macromolecules, which occurs in the interior of organic matter and the surface of minerals. The content of free oil is the main factor determining the mobility of shale oil. The 2D NMR spectrum shows that the selected samples have low organic matter content and high oil saturation, which is reflected in the weak signal of solid organic matter ($T_1 > 10$ ms and $T_2 < 0.2$ ms) and strong signal of crude oil ($T_1 > 10$ ms and $T_2 > 0.2$ ms). According to the mobility of the fluid, the crude oil is divided into three parts: heavy (0.2 ms $< T_2 <$ 2 ms), medium (2 ms $\leq T_2 <$ 20 ms) and light ($T_2 \geq$ 20 ms). The light part mainly represents light oil. The main components of heavy oil are colloid and asphaltene. The medium part is between the two. The light part is the amount of movable oil in reality (free shale oil), and the light + medium part (adsorbed-free shale oil) represent the maximum amount of movable oil. The heavy part is mainly the amount of immovable oil (adsorbed shale oil). The overall content of non-hydrocarbon and asphaltene of $P_2l_1^2$ is high (distributed between 15.39% and 72.77%, with an average of 34.65%) (Li et al., 2020a; Wang et al., 2021b), so the oil quality is relatively heavy. Previous studies have shown that the use of ultrasound on high viscosity crude oil is not as effective as that on low viscosity crude oil (Hamida and Babadagli, 2008; Mohammadian et al., 2012; Hamidi et al., 2014). Therefore, the samples with the

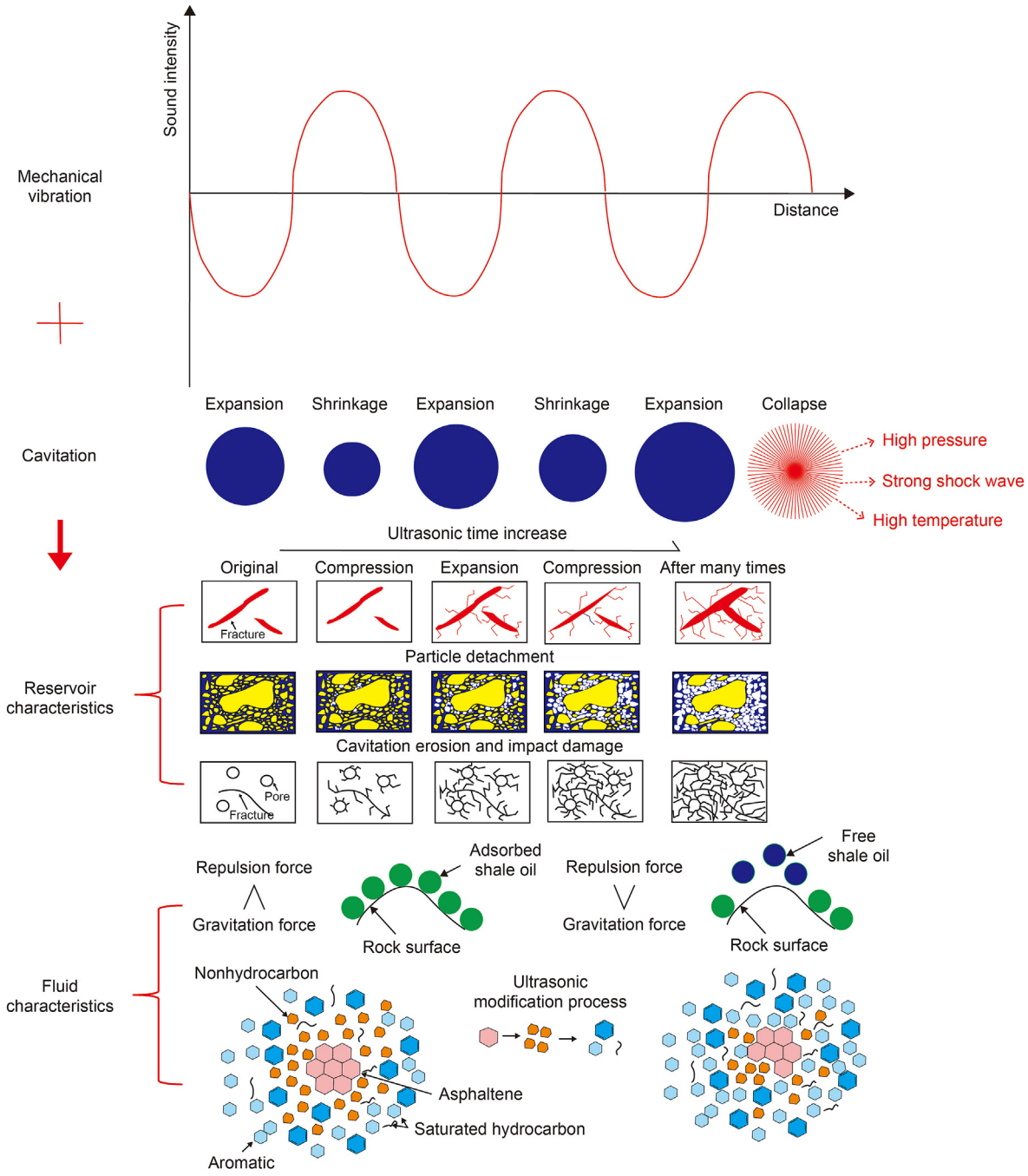

Fig. 8. Response characteristics of shale oil reservoir under ultrasonic.

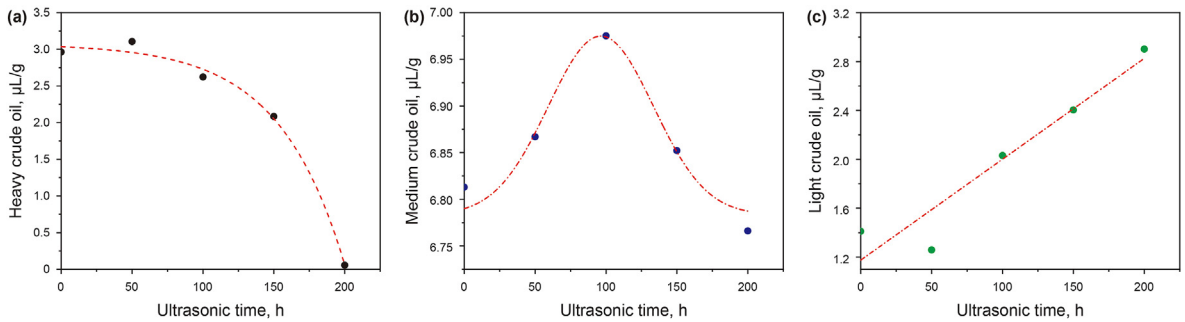

Fig. 9. Relationship between different kinds of crude oil and ultrasonic time.

best fluidity of $P_2l_1^2$ were selected (Figs. 1d and 5).

To more accurately describe the relationship between different crude oils and ultrasonic time, normalized fluid quantitative processing was carried out. The results show that with the increase of ultrasonic treatment time, the adsorbed-free shale oil changes to free shale oil as a whole. It is mainly reflected in the gradual decrease of adsorbed shale oil (Fig. 9a), the gradual increase of free shale oil (Fig. 9c), and the trend of first increase and then decrease of adsorbed-free shale oil (Fig. 9b), suggesting that there is gradual enhancement of shale oil fluidity under the action of ultrasonic waves. The reasons for ultrasonic effect to reduce viscosity and promote flow are as follows: 1) The collapse of cavitation bubbles generated by the ultrasonic waves will produce extreme conditions such as jets with a speed of 400 km/h. This extreme condition can instantly break the major molecules of heavy oil into light hydrocarbons, and it makes it impossible to restore the viscosity of heavy oil to the initial state (Lu and Zhang, 2004; Gopinath et al., 2006; Wang et al., 2006, 2018; Hamidi et al., 2014). In addition, the acoustic pressure change caused by cavitation can eliminate gas resistance and improve shale oil fluidity. In the actual reservoir, there are bubbles with various pore sizes (mainly composed of natural gas), which mainly exist in the form of gas nuclei. The existence of such gas nuclei has large obstacles to the flow of crude oil, which is referred to gas resistance. When the vibration frequency of the gas nuclei is close to that of the ultrasonic waves, a large number of gas nuclei form a large number of bubbles to achieve the effect of shedding capillary force. At the same time, the bubbles are broken under the action of cavitation to eliminate the gas resistance (Lu et al., 2002). 2) The mechanical oscillations of the ultrasonic effect causes the skeleton and particles of shale oil reservoir produce frequent reciprocating vibration. When the vibration frequency is close to that of shale oil molecules, the same frequency vibration will help shale oil molecules fall off the gravitational bondage, that is, reduce the affinity between crude oil and rock (Agi et al., 2019; Wang et al., 2020; Hamidi et al., 2021). Wu (2014) confirmed that when the ultrasonic power reached a certain value, the adsorbed molecules could get rid of the adsorption effect and become free molecules by calculating the adsorption mechanical parameters of shale and the reflected energy at the interface of ultrasonic waves. 3) When ultrasonic waves propagate in shale oil, the relative motion between shale oil molecules becomes more intense, resulting in the friction force of relative motion. When the friction force exceeds the force required for C–C bond breaking, macromolecular chains such as gum and asphaltene can be broken, so as to reduce the viscosity and enhance the fluid flow performance (Wang et al., 2018, 2020; Wang, 2019) (Fig. 8).

5.2.2. Increase imbibition recovery by pore-expanding effect

The NMR T_2 spectra of original samples after saturated oil showed bimodal distribution (the peak corresponding to T_2 were 0.2–0.4 ms and 80–100 ms, referred to as left and right peaks). With the increase of ultrasonic time, the double peaks of T_2 spectrum of the sample saturated with oil showed the following changes (the left peak gradually becomes “short and fat”, and the right peak gradually becomes “tall and thin”) (Fig. 7d). It showed that the relatively large pores of shale oil reservoir expanded, the pore types tended to be consistent, and the pore heterogeneity decreased after the ultrasonic treatment. In larger pores, it was easier for deuterium oxide to enter the reservoir and replace crude oil, the main imbibition driving force of this type of pores was gravity, and the imbibition mode was mainly forward imbibition, so the imbibition recovery was relatively high. For micro pores, the number decreases after the ultrasonic treatment. The capillary force as the main driving force of imbibition was weaker, and the main way of imbibition was reverse imbibition. Therefore, the crude oil in such pores was relatively difficult to extract, and the imbibition recovery was relatively low (Gu et al., 2019). Under the actual formation conditions, the stress of rock and its internal fluid is in a balanced state. When the ultrasonic waves act with high frequency and high periodicity, the balance is damaged. The change of pressure will lead to the periodic expansion and contraction of capillary pore size and pressure. Repeated extrusion is conducive to the flow of retained crude oil (Hamidi et al., 2021). When the impact pressure provided by ultrasound is large enough, the resistance effect of capillaries will be destroyed, and the pore-expanding effect is also conducive to the improvement of oil recovery. In addition, the spontaneous imbibition increased after the ultrasonic treatment, indicating that the reservoir water wettability is enhanced, which is also conducive to improving the imbibition recovery (Fig. 6).

6. Conclusion

(1) Under ultrasonic loading, the pore-fracture and pore connectivity of shale oil reservoir increased. The improvement of reservoir physical properties was mainly affected by ultrasonic mechanical vibration and cavitation. The main failure forms were particle detachment, fatigue damage and mechanical weak surface impact damage.

(2) After the ultrasonic treatment, the adsorbed-free shale oil changed to free shale oil, and the fluidity of fluid was enhanced. The cavitation and mechanical shear effect of ultrasound could make long-chain molecules split into multiple short-chain molecules, to reduce the viscosity and increase the fluidity of the fluid. In addition, the co-frequency vibration of shale oil molecules induced by the mechanical oscillations of the ultrasonic waves was also helpful for the adsorbed shale oil to fall off the gravitational bondage and transform to the free oil.

(3) Pore-expanding effect and fluid mobility enhancement are essential aspects of the power ultrasonic loading to improve the recovery of low mature shale oil.

Declaration of competing interest

No conflict of interest exits in the submission of this manuscript entitled “Mechanism of ultrasonic strengthening fluidity of low mature shale oil: A case study of the first member of Lucaogou Formation, western Jimusaer Sag, Northwest China”, and manuscript is approved by all authors for publication. I would like to declare on behalf of my co-authors that the work described was original research that has not been published previously, and not under consideration for publication elsewhere, in whole or in part. All the authors listed have approved the manuscript that is enclosed.

Acknowledgements

This project funded by National Natural Science Foundation of China (Grant No. U2244207, 42002186), Superior Youngth Foundation of Heilongjiang Province (YQ2021D004), Postdoctoral Science Foundation of Heilongjiang Province (LBH-Z20117) and Northeast Petroleum University Guiding Innovation Fund (2021YDL-02).

References

Agi, A., Junin, R., Shirazi, R., Gbadamosi, A., Yekeen, N., 2019. Comparative study of ultrasound assisted water and surfactant flooding. J. King Saud Univ. Sci. 31, 296–303. https://doi.org/10.1016/j.jksues.2018.01.002.

Bai, L., Liu, B., Du, Y., Wang, B., Tian, S., Wang, L., Xue, Z., 2022. Distribution characteristics and oil mobility thresholds in lacustrine shale reservoir: insights from N_2 adsorption experiments on samples prior to and following hydrocarbon extraction. Petrol. Sci. 19, 486–497. https://doi.org/10.1016/j.petsci.2021.10.018.

Cao, G., Lin, M., Ji, L., Jiang, W., Yang, M., 2019. Characterization of pore structures and gas transport characteristics of Longmaxi shale. Fuel 258, 116146. https://doi.org/10.1016/j.fuel.2019.116146.

Chen, J., Cheng, W., Wang, G., Li, H., 2021. Correlation mechanism between the law of ultrasonic propagation in coal samples and the migration of water. Fuel 310, 122264. https://doi.org/10.1016/j.fuel.2021.122264.

Dehshibi, R.R., Mohebbi, A., Riazi, M., Danafar, F., 2019. Visualization study of the effects of oil type and model geometry on oil recovery under ultrasonic irradiation in a glass micro-model. Fuel 239, 709–716. https://doi.org/10.1016/j.fuel.2018.11.071.

Dular, M., Osterman, A., 2008. Pit clustering in cavitation erosion. Wear 265 (5), 811–820. https://doi.org/10.1016/j.wear.2008.01.005.

Gopinath, R., Dalai, A., Adjaye, J., 2006. Effects of ultrasound treatment on the upgradation of heavy gas. Oil. Energ. Fuel. 20 (1), 271–277. https://doi.org/10.1021/ef050231x.

Gu, Y., Yu, G., Li, G., 2019. Experimental of pore structure and spontaneous imbibition of low permeability tight sandstone reservoirs. Sci. Technol. Eng. 19 (32), 139–145. CNKI:SUN:KXJS.0.2019-32-022.

Hamida, T., Babadagli, T., 2008. Fluid-fluid interaction during miscible and immiscible displacement under ultrasonic waves. Eur. Phys. J. B 62 (4), 515. https://doi.org/10.1140/epjb/e2008-00191-0.

Hamidi, H., Haddad, A.S., Otumudia, E.W., Rafati, R., Mohammadian, E., Azdarpour, A., Pilcher, W.G., Fuehrmann, P.W., Sosa, L.R., Cota, N., Garcia, D.C., Ibrahim, R.M., Damiev, M., Tanujaya, E., 2021. Recent applications of ultrasonic waves in improved oil recovery: a review of techniques and results. Ultrasonics 110, 106288. https://doi.org/10.1016/j.ultras.2020.106288.

Hamidi, H., Mohammadian, E., Junin, R., Rafati, R., Azdarpour, A., Junid, M., Savory, R.M., 2014. The effect of ultrasonic waves on oil viscosity. Petrol. Sci. Technol. 32 (19), 2387–2395. https://doi.org/10.1080/10916466.2013.831873.

Karr, U., Schuller, R., Fitzka, M., Denk, A., Strauss, A., Mayer, H., 2017. Very high cycle fatigue testing of concrete using ultrasonic cycling. Mater. Test. 59 (5), 438–444. https://doi.org/10.3139/120.111021.

Li, E., Xiang, B., Liu, X., Zhou, N., Pan, C., Dilidaer, R., Mi, J., 2020a. Study on the genesis of shale oil thickening in Lucaogou Formation in jimsar sag, junggar basin. Nat. Gas Geosci. 31, 250–257. https://doi.org/10.11764/j.issn.1672-1926.2019.09.003.

Li, W., Lu, S., Xue, H., Zhang, P., Hu, Y., 2016. Microscopic pore structure in shale reservoir in the argillaceous dolomite from the Jianghan Basin. Fuel 181, 1041–1049. https://doi.org/10.1016/j.fuel.2016.04.140.

Li, X., Cai, J., Liu, H., Zhu, X., Li, Z., Liu, J., 2020b. Characterization of shale pore structure by successive pretreatments and its significance. Fuel 269, 117412. https://doi.org/10.1016/j.fuel.2020.117412.

Liu, B., Bai, L., Chi, Y., Jia, R., Fu, X., Yang, L., 2019. Geochemical characterization and quantitative evaluation of shale oil reservoir by two-dimensional nuclear magnetic resonance and quantitative grain fluorescence on extract: a case study from the Qingshankou Formation in Southern Songliao Basin, northeast. Mar. Petrol. Geol. 109, 561–573. https://doi.org/10.1016/j.marpetgeo.2019.06.046.

Liu, B., Bechtel, A., Gross, D., Fu, X., Li, X., Sachsenhofer, R.F., 2018. Middle Permian environmental changes and shale oil potential evidenced by high-resolution organic petrology, geochemistry and mineral composition of the sediments in the Santanghu Basin, Northwest China. Int. J. Coal Geol. 185, 119–137. https://doi.org/10.1016/j.coal.2017.11.015.

Liu, B., Yang, Y., Li, J., Chi, Y., Li, J., Fu, X., 2020. Stress sensitivity of tight reservoirs and its effect on oil saturation: a case study of Lower Cretaceous tight clastic reservoirs in the Hailar Basin, Northeast China. J. Pet. Sci. Eng. 184, 106484. https://doi.org/10.1016/j.petrol.2019.106484.

Liu, Y., Dai, F., 2021. A review of experimental and theoretical research on the deformation and failure behavior of rocks subjected to cyclic loading. J. Rock. Mech. Geotech. 13 (5), 1203–1230. https://doi.org/10.1016/j.jrmge.2021.03.012.

Lu, B., Guan, J., Zhang, J., 2002. The application of pohlmann's whistle on crude oil wax control and viscosity reduction. Phys 31 (8), 517–520. https://doi.org/10.3321/j.issn:0379-4148.2002.08.008.

Lu, B., Zhang, J., 2004. Research of ultrosonic siren sound generator in wax proof and viscosity reduction. Oil Field Equipment 33 (1), 74–76. https://doi.org/10.3969/j.issn.1001-3482.2004.01.027.

Mohammadian, E., Junin, R., Rahmani, O., Idris, A.K., 2012. Effects of sonication radiation on oil recovery by ultrasonic waves stimulated water-flooding. Ultrasonics 53, 607–614. https://doi.org/10.1016/j.ultras.2012.10.006.

Mullakaev, M.S., Abramov, V.O., Abramova, A.V., 2015. Development of ultrasonic equipment and technology for well stimulation and enhanced oil recovery. J. Petrol. Sci. Eng. 125, 201–208. https://doi.org/10.1016/j.petrol.2014.10.024.

Otumudia, E., Hamidi, H., Jadhawar, P., Wu, K., 2022. Effects of reservoir rock pore geometries and ultrasonic parameters on the removal of asphaltene deposition under ultrasonic waves. Ultrason. Sonochem. 83, 105949. https://doi.org/10.1016/j.ultsonch.2022.105949.

Pawar, I.A., Joshi, P.J., Kadam, A.D., Pande, N.B., Kamble, P.H., Hinge, S.P., Banerjee, B.S., Mohod, A.V., Gogate, P.R., 2014. Ultrasound-based treatment approaches for intrinsic viscosity reduction of polyvinyl pyrrolidone (PVP). Ultrason. Sonochem. 21 (3), 1108–1116. https://doi.org/10.1016/j.ultsonch.2013.12.013.

Peng, C., Zhang, C., Li, Q., Zhang, S., Su, Y., Lin, H., Fu, J., 2021a. Erosion characteristics and failure mechanism of reservoir rocks under the synergistic effect of ultrasonic cavitation and micro-abrasives. Adv. Powder Technol. 32, 4391–4407. https://doi.org/10.1016/j.apt.2021.09.046.

Peng, S., Zha, X., Lei, X., Fei, F., Xu, D., Gao, Y., 2021b. Evolution characteristics and difference evaluation of shale oil reservoirs in the upper sweet spot interval of Lucaogou Formation in jimusaer sag. Special Oil Gas Reservoirs 28 (4), 30–38. https://doi.org/10.3969/j.issn.1006-6535.2021.04.005.

Pu, C., Shi, D., Zhao, S., Xu, H., Shen, H., 2011. Technology of removing near wellbore inorganic scale damage by high power ultrasonic treatment. Petrol. Explor. Dev. 38 (2), 243–248. https://doi.org/10.1016/S1876-3804(11)60030-X.

Razavifar, M., Qajar, J., 2020. Experimental investigation of the ultrasonic wave effects on the viscosity and thermal behaviour of an asphaltenic crude oil. Chem. Eng. Process 153, 107964. https://doi.org/10.1016/j.cep.2020.107964.

Sahinoglu, E., Uslu, T., 2015. Effects of various parameters on ultrasonic comminution of coal in water media. Fuel Process. Technol. 137, 48–54. https://doi.org/10.1016/j.fuproc.2015.03.028.

Shi, Q., Qin, Y., Li, J., Wang, Z., Zhang, M., Song, X., 2017. Simulation of the crack development in coal without confining stress under ultrasonic wave treatment. Fuel 205, 222–231. https://doi.org/10.1016/j.fuel.2017.05.069.

Shi, Q., Qin, Y., Zhou, B., Wang, X., 2019. Porosity changes in bituminous and anthracite coal with ultrasonic treatment. Fuel 255, 1–8. https://doi.org/10.1016/j.fuel.2019.115739.

Tang, Z., Zhai, C., Zou, Q., Qin, L., 2016. Changes to coal pores and fracture development by ultrasonic wave excitation using nuclear magnetic resonance. Fuel 186, 571–578. https://doi.org/10.1016/j.fuel.2016.08.103.

Wang, B., Liu, B., Sun, G., Bai, L., Chi, Y., Liu, Q., Liu, M., 2021b. Evaluation of the shale oil reservoir and the oil enrichment model for the first member of the Lucaogou Formation, western jimusaer depression, junggar basin, NW China. ACS Omega 6 (18), 12081–12098. https://doi.org/10.1021/acsomega.1c00756.

Wang, B., Liu, B., Yang, J., Bai, L., Li, S., 2022a. Compatibility characteristics of fracturing fluid and shale oil reservoir: a case study of the first member of Qingshankou Formation, northern Songliao Basin, Northeast China. J. Petrol. Sci. Eng. 211, 110161. https://doi.org/10.1016/j.petrol.2022.110161.

Wang, H., Li, H., Tang, L., Ren, X., Meng, Q., Zhu, C., 2022b. Fracture of two three-dimensional parallel internal cracks in brittle solid under ultrasonic fracturing. J. Rock. Mech. Geotech. 14 (3), 757–769. https://doi.org/10.1016/j.jrmge.2021.11.002.

Wang, J., Zhou, L., Jin, J., Liu, J., Chen, C., Jiang, H., Zhang, B., 2021a. Pore structure, hydrocarbon occurrence and their relationship with shale oil production in Lucaogou Formation of jimsar sag, junggar basin. Petrol. Geo. Expler. 43 (6), 941–948. https://doi.org/10.11781/sysydz202106941.

Wang, Y., 2019. Study on Key Technology of Viscosity Reduction of Heavy Oil by Ultrasound-Electromagnetic Dual Effect. Xian Shiyou University, Xian (in Chinese).

Wang, Z., Cheng, Y., Wang, G., Ni, G., Wang, L., 2022c. Comparative analysis of pore structure parameters of coal by using low pressure argon and nitrogen adsorption. Fuel 309, 122120. https://doi.org/10.1016/j.fuel.2021.122120.

Wang, Z., Fang, R., Guo, H., 2020. Advances in ultrasonic production units for enhanced oil recovery in China. Ultrason. Sonochem. 60, 104791. https://doi.org/10.1016/j.ultsonch.2019.104791.

Wang, Z., Gu, S., Zhou, L., 2018. Research on the static experiment of super heavy crude oil demulsification and dehydration using ultrasonic wave and audible sound wave at high temperatures. Ultrason. Sonochem. 40, 1014–1020. https://doi.org/10.1016/j.ultsonch.2017.08.037.

Wang, Z., Huang, J., 2018. Research on removing reservoir core water sensitivity using the method of ultrasound-chemical agent for enhanced oil recovery. Ultrason. Sonochem. 42, 754–758. https://doi.org/10.1016/j.ultsonch.2017.12.046.

Wang, Z., Wang, H., Guo, Q., 2006. Effect of ultrasonic treatment on the properties of petroleum coke oil slurry. Energy Fuel. 20 (5), 1959–1964. https://doi.org/10.1021/ef060144k.

Wang, Z., Xu, Y., 2015. Review on application of the recent new high-power ultrasonic transducers in enhanced oil recovery field in China. Energy 89, 259–267. https://doi.org/10.1016/j.energy.2015.07.077.

Wu, C., 2014. Mechanism and Experimental Study of Ultrasonic Promoting Shale Gas Desorption and Improving Seepage Characteristics. Southwest Petroleum University, Chengdu (in Chinese). https://kns.cnki.net/KCMS/detail/detail.aspx?dbname=CMFD201501&filename=1014409688.nh.

Xiao, D., Gao, Y., Peng, S., Wang, M., Lu, S., 2021. Classification and control factors of pore-throat systems in hybrid sedimentary rocks of Jimusar Sag, Junggar Basin, NW China. Petrol. Explor. Dev. 48 (4), 719–731. https://doi.org/10.1016/S1876-3804(21)60070-8.

Zhang, J., Li, Y., 2017. Ultrasonic vibrations and coal permeability: laboratory experimental investigations and numerical simulations. Int. J. Min. Sci. Technol. 27 (2), 221–228. https://doi.org/10.1016/j.ijmst.2017.01.001.